Nuclear Engineering and Design 280 (2014) 233–250

Contents lists available at ScienceDirect

Nuclear Engineering and Design

journal homepage: www.elsevier.com/locate/nucengdes

International benchmark study of advanced thermal hydraulic safety analysis codes against measurements on IEA-R1 research reactor

A. Hainoun[a,*], A. Doval[b], P. Umbehaun[c], S. Chatzidakis[d], N. Ghazi[a], S. Park[e], M. Mladin[f], A. Shokr[g]

[a] Atomic Energy Commission of Syria (AECS), Nuclear Engineering Department, P.O. Box 6091, Damascus, Syrian Arab Republic
[b] Nuclear Engineering Department, Av. Cmdt. Luis Piedrabuena 4950, C.P. 8400 S.C de Bariloche, Rio Negro, Argentina
[c] Centro de Engenharia Nuclear – CEN, IPEN-CNEN/SP, Av. Lineu Prestes 2242-Cidade Universitaria, CEP-05508-000 São Paulo, SP, Brazil
[d] School of Nuclear Engineering, Purdue University, West Lafayette, IN 47907, United States
[e] Research Reactor Design & Engineering Division, Basic Science Project Operation Dept., Korea Atomic Energy Research Institute, Republic of Korea
[f] Institute for Nuclear Research, Campului Street No. 1, P.O. Box 78, 115400 Mioveni, Arges, Romania
[g] Division of Nuclear Installation Safety, Research Reactor Safety Section, International Atomic Energy Agency, A-1400 Vienna, Austria

HIGHLIGHTS

- A set of advanced system thermal hydraulic codes are benchmarked against IFA of IEA-R1.
- Comparative safety analysis of IEA-R1 reactor during LOFA by 7 working teams.
- This work covers both experimental and calculation effort and presents new out findings on TH of RR that have not been reported before.
- LOFA results discrepancies from 7% to 20% for coolant and peak clad temperatures are predicted conservatively.

ARTICLE INFO

Article history:
Received 14 January 2014
Received in revised form 26 June 2014
Accepted 29 June 2014

ABSTRACT

In the framework of the IAEA Coordination Research Project on “Innovative methods in research reactor analysis: Benchmark against experimental data on neutronics and thermal hydraulic computational methods and tools for operation and safety analysis of research reactors” the Brazilian research reactor IEA-R1 has been selected as reference facility to perform benchmark calculations for a set of thermal hydraulic codes being widely used by international teams in the field of research reactor (RR) deterministic safety analysis. The goal of the conducted benchmark is to demonstrate the application of innovative reactor analysis tools in the research reactor community, validation of the applied codes and application of the validated codes to perform comprehensive safety analysis of RR. The IEA-R1 is equipped with an Instrumented Fuel Assembly (IFA) which provided measurements for normal operation and loss of flow transient. The measurements comprised coolant and cladding temperatures, reactor power and flow rate. Temperatures are measured at three different radial and axial positions of IFA summing up to 12 measuring points in addition to the coolant inlet and outlet temperatures. The considered benchmark deals with the loss of reactor flow and the subsequent flow reversal from downward forced to upward natural circulation and presents therefore relevant phenomena for the RR safety analysis.

The benchmark calculations were performed independently by the participating teams using different thermal hydraulic and safety analysis codes that comprise of CATHARE, RELAP5, MERSAT and PARET. The code RELAP5 was used independently by four of the participating teams and therefore the user effect and its impact on the code results can be characterized. The benchmark results demonstrate that most of the codes have the capability to correctly predict the SS case. However, for the LOFA case the simulation results show discrepancies to the measurement although the majority of the applied codes predict a qualitative correct time evolution of the corresponding transients for the coolant and clad temperatures. It is noted that the peak temperatures and the gradients around them are predicted conservatively. The quantitative assessments of benchmark results indicate different amounts of discrepancy between

* Corresponding author. Tel.: +963 112132580; fax: +963 6111926/7.
E-mail address: pscientific2@aec.org.sy (A. Hainoun).

http://dx.doi.org/10.1016/j.nucengdes.2014.06.041

predictions and measurements ranging between 7% and 20% for peak clad temperatures during LOFA. The comparative prediction capability of the employed codes is addressed by additional code-to-code comparisons based on selected TH parameters that comprise flow rate, pressure drop and heat transfer coefficient during natural circulation phase.

1. Introduction and background

The qualification of an integrated set of thermal hydraulic–neutronics codes is essential for performing comprehensive research reactors safety analysis that considers the coupled interaction of thermal hydraulic and neutronic phenomena. Thus, the ultimate task of the performed research activities in this CRP aimed at assessing the capabilities and determining the suitability of various thermal hydraulic codes for the application in design, operation and safety analysis of research reactors (RR).

During the last two decades intensive effort has been undertaken to develop, modify and validate advanced computational tools for application in the safety analysis of RR. A number of modelling tools have been adopted from the area of nuclear power reactors and were further extended to account for the special design and operation features of RR. Prominent for this class of tools are the system thermal hydraulic (SYS-TH) codes like RELAP, CATHARE, ATHLET and MERSAT that are able to model the whole rector system and have meanwhile special versions for the application on RR. Besides, other relatively simpler tools like PARET and PLTEMP-ANL were originally developed for the application on RR. They are limited to model part of the reactor core or selected fuel assemblies and remain useful for application on simple transients where special phenomena are investigated. However, for complex transients or accidents such as reactivity insertion accident (RIA), loss of flow accident (LOFA) and loss of coolant accident (LOCA) where coupled neutronic–thermal hydraulic phenomena are expected to occur and various parts of reactor facility are involved, advanced system codes are required to address the expected physical phenomena.

Early adopted conservative modelling assumptions in the reactor safety analysis – based on assessment of worst case scenarios – have been replaced by "best-estimate" methodologies. The best-estimate approach aims at providing a detailed realistic description of postulated accident scenarios based on best-available modelling methodologies and numerical solution strategies sufficiently verified against experimental data from differently scaled separate and integral effect test facilities (Bestion, 2008; D'Auria and Mazzantini, 2010). Subsequent to achieving an extensive validation process and reaching high quality of prediction the above mentioned SYS-TH codes are meanwhile classified as best-estimate system codes and being considered as qualified for application in licensing processes of nuclear power reactors.

Nevertheless, due to the fact that the above mentioned SYS-TH codes have been originally developed and validated for the application on power reactors, the extension of their application to the safety analyses of RRs require additional development and validation efforts to cope with the specific features of RR (Hainoun et al., 1996; Hainoun and Schaffrath, 2001). Furthermore, the increased extensive use of research reactor together with the augmented safety requirements, has enlarged the necessity to get more realistic simulations of the phenomena involved during steady-state and transient conditions and eventually the identification of design/safety requirements that can be relaxed or enhanced (D'Auria et al., 2004; Benchmark, 2014). In this regard, acknowledgeable effort has been done from various international teams to validate such codes using separate effect tests. RELAP and ATHLET as prominent example of SYS-TH codes undergone extensive extension and validation for the application on RR safety. ATHLET was extended and validated to cover TH flow instability for the cases of low and high power RR (Hainoun and Schaffrath, 2001). RELAP5 is meanwhile widely used for RR analysis. Thus, many teams work on its extension, validation and application for RR safety analysis (Hamidouche and Bousbia-Salah, 2006; Hamidouche et al., 2008, 2009; Omar et al., 2010). The same trend can be observed for the codes CATHARE, MERSAT and PARCS (Hainoun and Schaffrath, 2001; Hainoun et al., 1993). New trend is observed during the last years aiming at coupling 3-D neutron kinetic to the SYS-TH codes to replace existing point kinetic model and thus to improve the code predictability in case of reactivity insertion accident where 3-D effects are important (Hamidouche et al., 2009). Although such effort are of great importance for improving the code capability, its validation remains challengeable due to the lack of adequate integral effect test where TH and neutron kinetic effects are dynamically interlinked. In fact recent attempt to validate SYS-TH codes for the simulation of fast and large reactivity insertion in RR using SPERT-IV experiments show limited success. In particular for large reactivity insertion codes predictions largely overestimate measured peaks for power and clad temperatures corresponding to possible deficit in tackling reactivity feedback effects related to fast transients (Day and Chatzidakis, 2012).

Moreover, the IAEA accomplish in 2008 a CRP project to validate SYS-TH codes against separate effect tests that covered void fraction distribution, single and two phase pressure losses, heat transfer coefficients and TH flow instability (Safety report, 2008). Unfortunately and in contrast to power reactor, RR safety analysis suffers from the lack of data base to perform code qualification based on integral effect tests. This contribution aims – on one side – to give an example for integral effect benchmarking of various advanced TH codes for the application on RR and on the other side to point to the deficit in the quality of rarely available real integral RR experiments. This can be very useful in supporting future effort to define international benchmark problems – and establish the required integral test – for the purpose of RR qualification.

It should be mentioned that this contribution shall not be considered as qualification of SYS-TH codes. It is rather a good step in this direction. It gives the RR safety community an example how an international effort can be accomplished to benchmark advanced SYS-TH codes against integral effect test and to demonstrate how common effort can be useful to share knowledge and exchange experiences among international teams on the way of qualifying such codes.

In line with above mentioned requirements, instrumented fuel assemblies (IFA) present a valuable tool to acquire integral effect tests required for the validation of SYS-TH codes on the way to their qualification for the design and safety analysis of RR. IFAs provide realistic data necessary both for understanding the reactor behaviour and for validating the computer codes in a passable benchmark process. In line with this approach, an IFA has been constructed and installed in the core of the Brazilian IEA-R1 MTR reactor. This IFA was designed for performing thermal hydraulic measurements under normal operation and during loss of flow transient/accident (LOFA). The IFA was positioned in two different locations in the reactor core and under different operational conditions. Different radial positions of IFA can also serve to account for the influence of radial power factors. Each of the two measurement sets comprises of 14 coolant and clad temperatures distributed in the radial and axial direction of IFA. The experimental data serve as a reference to benchmark the thermal hydraulic codes CATHARE, MERSAT, PARET and RELAP5. The computational tools have been used by seven teams from various countries participating in this international benchmark analysis, namely: Argentina, Bangladesh, Brazil, Greece, Romania, South Korea, and Syria. The goals of the conducted benchmark analyses can be summarized as follow:

- Application and support for further development of innovative reactor analysis tools in the research reactor community with the ultimate purpose of supporting the transfer of such tools to a larger research reactor community.
- Validation of the applied codes against experimental data, and application of the validated codes to simulate steady state and transients covering a variety of neutronic and thermal-hydraulic conditions for various selected research reactors.
- Application of the validated analysis tools in the safety analysis of RR.
- Completing the benchmark analysis by the code-to-code comparison for the same experimental sets in order to classify the confidence of the involved codes and identifying any user effects amongst the involved teams.

In addition to benchmarking against the IFA experimental data, the broad-spectrum of the employed codes enables the consideration of code-to-code comparison. This way, one can evaluate the codes capabilities to simulate the relevant TH phenomena and assess them regarding appropriateness for application in the safety analysis of RR.

It should be stressed that the considered benchmark analysis in this work deals with two related phenomena of the loss of reactor flow (LOFA) and the subsequent flow reversal from downward forced to upward natural circulation. Both phenomena are observed in downward cooled RR and characterized though relevant TH parameters of flow stagnation, flow reversal and natural circulation. Such phenomena present significant challenge for the fuel element integrity, in particular for the case when the reactor shutdown delays or even fails. Thus, for many downward cooled RR LOFA is classified in the group of design basis accident.

It is asserted that this work includes some novelty in experimental and computational senses. It covers new experimental data on TH of RR and comparative benchmarking of advanced codes being used by five independent international teams. Both efforts have not been reported before.

The structure of this contribution comprises a short description of the employed computer codes and the adopted approach to model the IEA-R1 reactor. The second step presents the benchmark results by comparing the code prediction with the experimental data and commenting on the observation. The comparison should allow for evaluating the prediction capability of the employed codes and indicate possible further development.

The last part is devoted to code-to-code comparison, where the results are compared for the purpose of comparative assessment to account for possible improvement of selected physical models in the employed codes. In addition, for the case of the RELAP5 code which is being used by various teams, the comparison of calculated results of all teams could also serve to evaluate the user effect. At this stage the impact of user experience and the applied modelling approach on the final code results can be evaluated and possible recommendation for future code application can be given.

Table 1
Participating teams and codes used for IEA-R1 benchmark analysis.

Working team	Applied code	Type of calculation
Argentina (ARG)	RELAP-5 mod 3.2	SS and LOFA
Brazil (BRZ)	PARET-ANL, MTRCR	SS
Greece (GRE)	RELAP5/MOD3.3	SS and LOFA
Romania (ROM)	CATHARE	SS and LOFA
South Korea (KOR)	RELAP	SS and LOFA
Syria (SYR)	MERSAT, RELAP	SS and LOFA

2. Description of applied codes

The thermal hydraulic codes CATHARE, MERSAT, RELAP and PARET have been applied for the analysis of IEA-R1. The codes have been used by six independent teams from different countries that participated in this international benchmark and consists of Argentina (RELAP5), Brazil (PARET-ANL and MTRCR), Greece (RELAP5), Romania (CATHARE), South Korea (RELAP5) and Syria (MERSAT, RELAP5) (Table 1). The first three codes CATHARE, MERSAT and RELAP5 belong to the advanced TH codes being able to model the main important thermal hydraulic phenomena related to the safety analysis of light water cooled reactors up to the level of design basis accident. They are based on a one dimensional (1-D) fluid dynamics approach with a comprehensive heat transfer package in the two phase flow regime. Detailed description and comparison of advanced SYS-TH codes is presented in Bestion (2008).

CATHARE (Code for Analysis of Thermal-Hydraulics during an Accident of Reactor and Safety Evaluation) is a best-estimate code developed initially to simulate PWR accidents (small and large break LOCAs and RIA) (Noel, 2011). The code is developed in France by CEA-Grenoble and is a joint effort of CEA, IRSN, EDF and AREVA_NP. The current version in INR Piteşti – which has a user license agreement signed with IRSN – is CATHARE2 V25-2 mod 8.1 (Lavialle; Bestion, 2008). CATHARE is based on six conservation equations for the two phase flow of water. The domain of parameters is from 0.1 to 25 MPa for pressure, from 20 °C to 2000 °C for gas temperature, and up to sonic condition for fluid flow. It uses an implicit integration method and can run with several parallel processors. It has the graphical user interface GUITHARE to perform pre- and post-processing.

MERSAT (Model for Evaluation of Reactor Safety and Analysis of Thermal hydraulic) is being developed and validated at the AECS (Hainoun et al., 2008a). It is classified among one-dimensional, two-phase fluid dynamic code for the thermal hydraulic safety analysis of light-water reactors during transients and loss of coolant accidents. The one-dimensional, two-phase fluid dynamic model is based on the conservation equations for the steam and water mass, mixture energy and the mixture momentum (4-equation). Mechanical non-equilibrium of the two phases is described in the momentum equation using the drift-flux model of Zuber & Findlay. Thermodynamic non-equilibrium of the two phases in the subcooled boiling regime is described with a sophisticated model that takes into consideration the competing evaporation and condensation effects in this regime. It describes the bubble generation rate at the superheated heating surfaces as well as the subsequent condensation of the bubbles in the sub cooled core flow (Hainoun and Alissa, 2005; Umbehaun et al., 2012; Safety report, 2008). MERSAT consists of several modules to dealing with two-phase fluid dynamics, heat conduction and heat transfer and nuclear heat generation using point-kinetics approach. The code includes also basic control component for modelling special hydrodynamic components, like fill, leak, time-dependent volume, etc. various single and integral effect tests have been performed to validate the code for the thermal hydraulic and safety analysis of research reactors (Hainoun et al., 2008a).

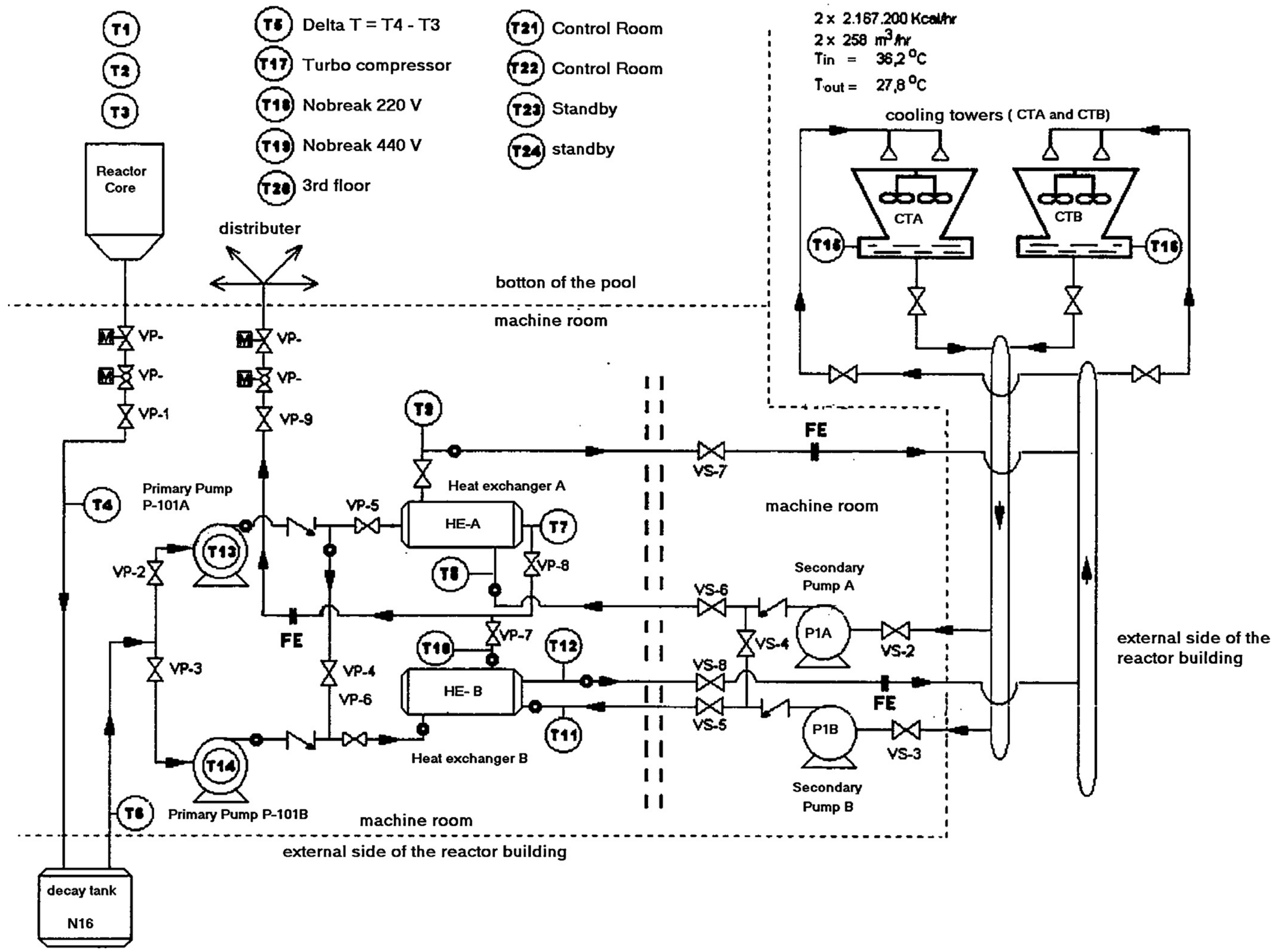

Fig. 1. Schematic process diagram of the IEA-R1 reactor (Umbehaun, 2012).

RELAP (Reactor Excursion and Leak Analysis Programme) is a system thermal hydraulics code used for the simulation of wide range of transients and accidents in water-cooled power reactors. It is based on coupled equations to model thermal hydraulic reactor coolant system and neutron kinetics of the reactor core (Bestion, 2008). The hydrodynamic model is one-dimensional two-phase flow which can contain non-condensable components in the vapour phase and/or a soluble component in the liquid phase (Nuclear Safety Analysis Division, 2001a, 2001b). The nuclear heat generation is simulated using the point kinetics approach. RELAP has been widely used around the world. Even though RELAP5 code system was first devoted for the analysis of nuclear power plants during the last two decades RELAP 5 has been increasingly used in the safety analysis of research reactors.

PARET-ANL was originally developed at INEL (Idaho National Engineering Laboratory) and later improved at ANL (Argonne National Laboratory). It is a widely used calculation tool for coupled neutronic, thermal-hydraulic simulations in research reactors. The code employs one-dimensional hydrodynamics, one-dimensional heat transfer and point kinetics with continuous reactivity feedback (Obenchain, 1969). A simplified void fraction model is included to estimate the void produced by sub-cooled boiling. Recently a sophisticated model to predict sub-cooled void formation for RR conditions has been included and validated by Hainoun et al. (2008b). The heat transfer along the fuel plate is calculated using a set of constitutive equations for two phase flow. PARET has been validated against experimental results of power transient tests from the SPERT experimental programme. The comparison with the measurements – of power and clad temperature – was generally favourable (Torres et al., 2003).

3. Description of IEA-R1 facility

In this section the IEA-R1 reactor facility is described with special focus on the specifications of the instrumented fuel assembly (IFA). More details with regard to IEA-R1 facility can be found in (Database of Research Reactor Benchmarks, 2014).

3.1. Description of IEA-R1 reactor

The IEA-R1 is a 5 MW open pool type research reactor using low enrichment MTR fuel assemblies. Fig. 1 shows a simplified scheme of the primary and secondary loops.

The reactor core is cooled by downward flow and the reactor heat removal is based on primary and secondary cooling systems. The pool water of the primary system is pumped downward through the fuel assemblies to remove the fission heat from the reactor core. A water to water heat exchanger transfers the generated heat to a secondary water cooling system. The secondary system carries heated water to the cooling tower which dissipates the heat to the atmosphere. The primary water is then returned to the reactor pool. Water from the cooling tower is re-circulated through the secondary system.

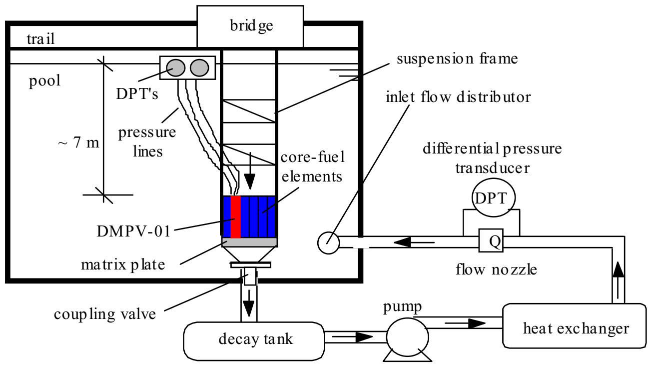

Fig. 2. Simplified illustration of primary system of IEA-R1.

By operating the reactor at 5 MW loop A is involved (Pump P-101A or P-101B, the Heat Exchanger HE-B, the Pump P1A or P1B and the Cooling Tower CTB). The other heat exchanger and cooling tower are used only for low power operation (<3 MW).

The primary cooling system of the IEA-R1 consists of a pool, piping, decay tank, pumps, heat exchangers, flow metre system, distributor, valves and structures, as schematically shown in Fig. 2. The primary pump circulates water through the core to remove the heat generated during the reactor operation. Then, the water flows through the decay tank to decrease the N16 activity before entering the pump and heat exchanger, which transfers the heat to the secondary cooling system.

To start operation a manually actuated pneumatic system lifts a device, named header, to couple the outlet nozzle to the core matrix plate. Then, the pump is turned on and the primary operating flow rate is adjusted to the pre-determined operating point. The pneumatic system is turned off and the device is kept coupled by hydrodynamic force resulting from the pressure difference. Subsequently, the reactor power operation is adjusted. If the primary flow rate decreases below the low flow set-point value (90%), the reactor is automatically shutdown and the coupling device falls by action of the gravity and then the residual heat is removed by natural circulation in the reactor pool (Umbehaun et al., 2012; Umbehaun, 2012).

Fig. 2 shows the location of reactor core inside the reactor pool. The total volume of water in the pool is around 272 m^3.

The reactor arrangement consists of fuel assemblies, beryllium reflectors, control rods and irradiation positions inside the reactor core. The core comprises standard 20 fuel assemblies, 4 control fuel assemblies and a central irradiator, assembled in a square matrix of 5 × 5. Each fuel element has 18 fuel plates assembled on two lateral support plates, forming 17 independent flow channels. The control fuel element includes only 12 plates as there are two dummy lateral plates and two guide channels for the control plates. Table 2 summarizes the main reactor design parameters.

3.2. Experiment description

To investigate the thermal hydraulic behaviour of the fuel assembly under normal and transient conditions, an IFA has been manufactured and installed in certain locations in the reactor core. The impact of radial peaking factors and different operational conditions on the thermal hydraulic behaviour of the fuel assembly is assessed by positioning the IFA at two different locations resulting in two experimental configurations (Fig. 3). In the configuration 243 the IFA was located at the outermost core corner (lower right) whereas in the configuration 246 the IFA was located on the midline left to the core centre.

Fig. 4 presents the IFA with the assigned measurements positions and Table 3 summarizes the assigned temperatures at the considered locations of the IFA thermocouples. The IFA has overall 14 thermocouples distributed as follows:

- 2 thermocouples for coolant inlet and outlet temperature,

Table 2
Description of design parameters of IEA-R1 research reactor (Umbehaun, 2012).

Reactor parameter	Data	Notes
Steady state power level (MW)	2–5	Depends on irradiation necessity
Fuel enrichment	<19.75%	
Number of fuel assembly in the core	24	
(a) Standard fuel assembly	20	
(b) Control fuel assembly	4	
Fuel types		
U_3O_8–Al	Density 2.3 g/cm^3	Mass U235 per fuel assembly 196.9 g
U_3Si_2–Al	Density 3.0 g/cm^3	Mass U235 per fuel assembly 275.5 g
Maximum inlet temperature (°C)	40	
ΔT_{core} at 5 MW	5.8 °C	Between inlet and outlet
Number of fuel plates in		
(a) Standard fuel assembly	18	
(b) Control fuel assembly	12	
Fuel meat dimensions (mm)	0.76 × 62.6 × 600	
Clad thickness (mm)	0.38	
Total width of the plates (mm)	67.1	
Fuel meat dimensions (mm)	0.76 × 62.6 × 600	
Thickness of water channel (mm)	2.89	
Water pool volume (m^3)	272	
Coolant flow rate (m^3/h)	Total: 772, one FA: 22.8 Core flow: 22.8 × 24 = 547.2 Bypass: 224.8	
Core pressure drop – normal condition	7.835 kPa	Measured
Pressure drop of primary system	400 kPa	Approximately
Uncertainties		
Deviation in fuel loading per plate	12%	
Fluctuation in uranium density	2%	
Error in meat thickness	10%	
Power measurement	5%	
Power density variation	10%	
Flow rate measurement	3%	

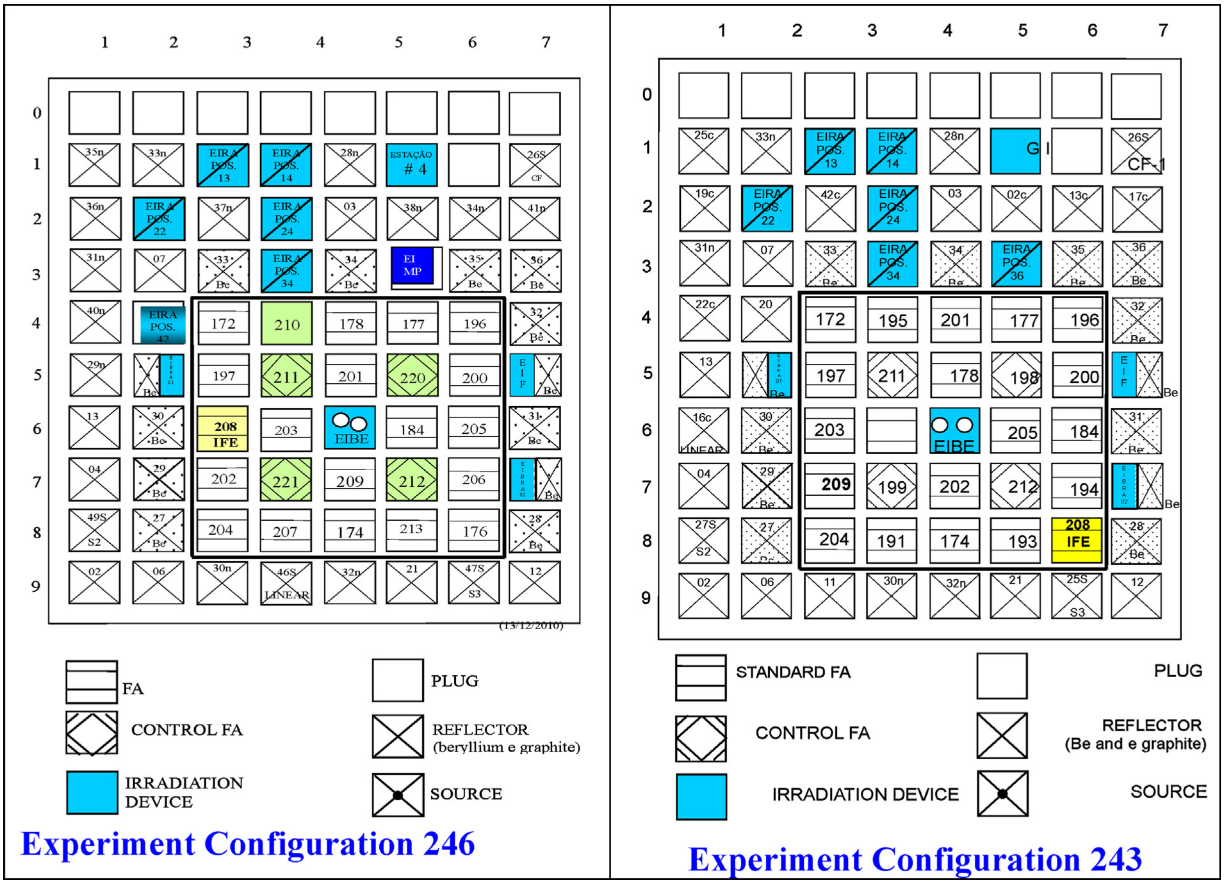

Fig. 3. Position of IFA for the 243 and 246 core configuration (IFE refers to IFA).

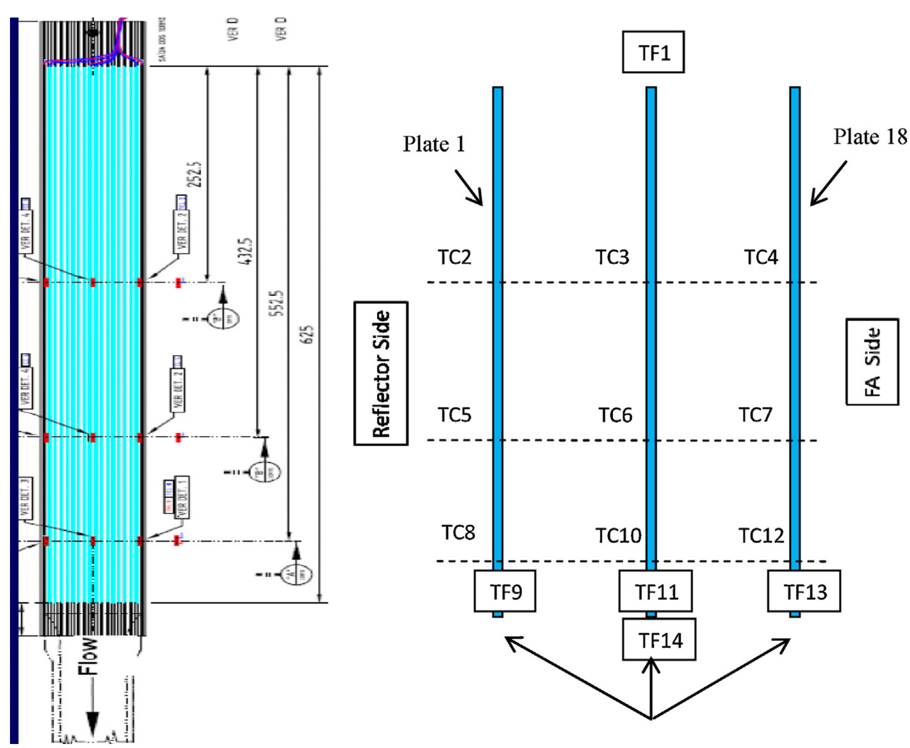

Fig. 4. Vertical section of instrumented fuel assembly.

Table 3
Locations and symbols of IFA thermocouples.

Position from channel entrance (mm)	Reflector side	Central	FA side
Clad temperatures			
252.5	TC2	TC3	TC4
432.5	TC5	TC6	TC7
552.5	TC8	TC10	TC12
Fluid temperatures			
552.5	TF9	TF11	TF13

TF1: fluid inlet temperature, TF14: fluid outlet temperature.

- three coolant channels, one central and two lateral, each equipped with 3 thermocouples for measuring cladding temperature and 1 thermocouple for measuring the coolant temperature.

The internal flow rate distribution inside the fuel assembly was measured in a previous work using a Dummy FA (Torres et al., 2003). The measurement indicated an approximately parabolic distribution across the cooling channel. Based on this work the distribution parameters of channel velocity to average FA velocity for the central channel, reflector side and FA side are 1.041, 0.91 and 0.885 respectively. This approach is applied to calculate the flow velocities of the three different FA zones, namely central, reflector side and fuel assembly side (Fig. 4). Hence, the distribution of IFA flow rate of 22.8 m^3/h on the 18 flow channels (17 internal and 2 half outer channels) of IFA gives an average channel velocity of 1.92 m/s (total flow area in channel region is 0.0033 m^2). Merging the channels in 3 groups, gives the resulting channels velocities of IFA as follow:

– central channel: 2 m/s,
– reflector side channel: 1.8 m/s,
– FA side: 1.65 m/s.

The axial power distributions along the 3 groups of channels have been provided by the reactor operator and presented in Fig. 5. Neutron kinetic data required to simulate reactor dynamic behaviour including nuclear heat generation are specified according to the supplied operator data (Database of Research Reactor Benchmarks, 2014).

The steady state boundary conditions are specified as follow:

◦ inlet pressure: 1.7 bar,
◦ nominal power: 3.5–5 MW,
◦ total flow rate (core and bypass): 211 kg/s,
◦ core inlet temperature: 32.7–40 °C,
◦ pool temperature: 32.7 °C.

The radial power peaking factor of the IFA was estimated from the experimental data of the steady state operation based on the underneath proposed approach. Another approach can be adopted subject to experimental data availability. The local power of the IFA (P_{IFA}) has been calculated using the available experimental data of coolant flow rate (G_{IFA}), inlet (T_{in}) and outlet (T_{out}) temperatures as follow:

$$P_{IFA} = G_{IFA} c_p (T_{out} - T_{in})$$

The resulting local power of the IFA and the corresponding radial peaking factors for the different reactor power levels are presented in Table 4.

3.3. Codes input models of IEA-R1

Different IEA-R1 input models have been developed using the adopted computational codes depending on the nodalization techniques of each code. The code users adopted different levels of detailed description of primary and secondary loops and reactor core. The developed models consist of inlet zone linked to the reactor inlet plenum, an active fuel zone with flow channel and output zones linked to the rector outlet plenum. To reflect radial and axial temperature distribution various sub-channels with adequate vertical discretization are applied. The majority of the developed models reduce the number of fuel assemblies by merging those having nearly similar power peaking factors. This approach helps in reducing calculation effort without compromising the simulation results for the transients considered in this analysis, as the benchmark focuses on the IFA. Thus, all codes imply a detailed modelling of the IFA that is described as a separate fuel element consisting of three parallel cooling channels corresponding to the radial zones of central, reflector and fuel assembly sides. For the three zones radial and axial power distribution as well radial velocity distribution are experimentally available (see Fig. 4). Fig. 6 represents the developed nodalization models of the IEA-R1 reactor using the applied codes and Table 5 summarizes their main input parameters. Detailed descriptions of the developed input models can be found in (Database of Research Reactor Benchmarks, 2014).

4. Results and discussion

4.1. Steady state (SS) benchmark results

The SS experimental data correspond to values averaged over the time interval immediately before starting the LOFA. For example, for the power level of 3.5 MW the temperatures are averaged over 70 s of measuring time. Table 6 summarizes the SS benchmark results for all codes for the 3.5 MW reactor power. It is observed that

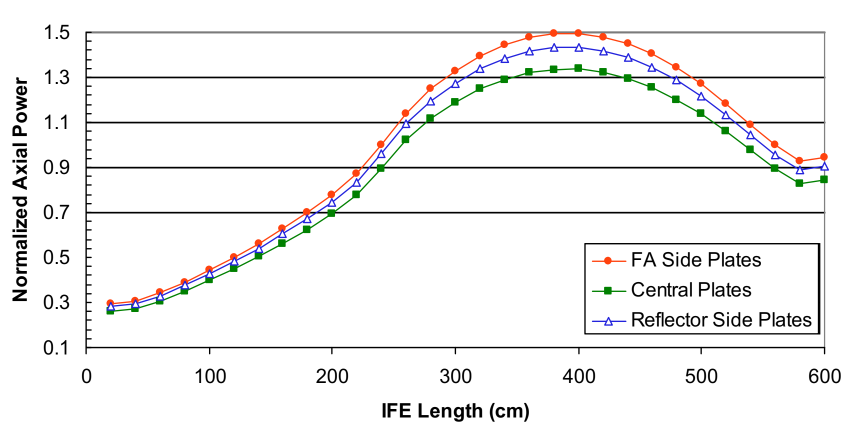

Fig. 5. Normalized axial power distribution for the IFA (configuration 243).

Table 4
Derived local IFA power based on measurements of flow rate, inlet and outlet coolant temperatures.

Reactor power (MW)	Experimental data			Derived parameters	
	Inlet (°C)	Outlet (°C)	Flow rate (kg/s)	IFA power (kW)	Radial power factor of IFA
3.5	32.69	37.57	6.27	128.0	0.829
4.0	31.61	37.23	6.27	147.4	0.835
4.5	32.53	38.69	6.27	161.6	0.814
5.0	33.43	40.21	6.27	177.68	0.805

For 3.5 MW:
Average power per plate: 3.5/(20 × 18 + 4 × 12) = 3.5/408 = 8.578 kW.
Average FA power, Pav = 18 × 8.578 = 154.4 kW.
Pfr = PIFA/Pav = 0.829.

Table 5
Main nodalization parameters of the developed IEA-R1 models.

Parameter	ARG-R	GRE-R	KOR-R	ROM-C	SYR-R	SYR-M
Nr. of core channels	5	5	5	20	26 + 1BYPASs	8 + 1BYPASS
IFA channels	3	3	3	18	3	3
Axial CV per channel	30	30	30	12	30: IFA 15: others	30: IFA 15: others
Nr. of heat structures	4	4	4	38	26	8
Axial CV per HS	30	20	30	12	30: IFA 15: others	30: IFA 15: others
Radial zones per fuel plat	2	7	10	3	16	3
Pool's CVs	2	4	4	4	10	10
Inlet plenum: Dh (m)	Pool dimensions	0.55	0.13	0.07	0.40	0.40
High (m)		0.20	0.05	0.15	0.50	0.50
Outlet plenum: Dh (m)	0.63	0.65	0.58	0.07	0.40	0.40
High (m)	0.65	0.23	0.27	0.15	0.27	0.27

CV: control volume, Dh: hydraulic diameter, IFA: instrumented fuel assembly, C: CATHARE, M: MERSAT, R: RELAP.

the agreement between calculation and measurement is better for the lateral than for the central positions. The absolute local difference of prediction against experiment varies between −5 °C and +8 °C corresponding to a maximum relative deviation of −12% and +21% respectively. The maximum discrepancy is observed at the central position of IFA (TC3). The high deviation trend is common to all teams which may identify a possible bias in the experimental data. For the quantitative assessment of the discrepancy between measurement and code prediction the average relative deviation (AVD) is defined as follows:

$$\mathrm{AVD} = \frac{1}{n}\sum_{i=1}^{n}\sqrt{\left(\frac{T_{\exp}-T_{cal}}{T_{\exp}}\right)^2}\cdot 100$$

Table 6
Benchmark results of the applied codes for the 3.5 MW SS OPERATIONS (configuration 243). [Diff. refers to the relative difference between experiment and prediction and AVD is the average relative difference over all benchmark results[a]].

T (°C)	Exp	ARG		BRZ				GRE		KOR		ROM		SYR			
		RELAP	Diff.	PARET	Diff.	MTRCR	Dif.	RELAP	Diff.	RELAP	Diff.	CATHARE	Diff.	MERSAT	Diff.	RELAP	Diff.
TC2	43.8	44.2	0.8%	46.0	4.9%	43.2	−1.5%	45.3	3.4%	42.6	−2.9%	46.8	6.8%	42.9	−2.1%	43.7	−0.4%
TC3	37.5	44.2	17.8%	42.7	13.9%	38.2	1.7%	44.4	18.2%	42.1	12.2%	45.5	21.2%	42.1	12.2%	44.3	18.2%
TC4	44.5	44.2	−0.7%	45.5	2.2%	42.2	−5.1%	46.0	3.3%	43.0	−3.4%	47.6	7.0%	43.1	−3.1%	43.7	−1.8%
TC5	48.0	52.6	9.6%	54.0	12.4%	49.5	3.0%	50.9	6.0%	48.5	0.9%	46.8	−2.5%	48.8	1.6%	48.1	0.1%
TC6	42.5	51.0	19.9%	48.8	14.7%	42.0	−1.3%	49.6	16.5%	47.8	12.2%	51.0	19.9%	47.4	11.4%	49.0	15.2%
TC7	49.2	53.5	8.8%	53.1	8.0%	47.8	−2.8%	51.7	5.2%	49.1	−0.1%	53.7	9.2%	49.1	−0.2%	48.5	−1.4%
TC8	45.2	50.4	11.5%	51.0	12.9%	47.4	4.8%	48.8	7.9%	46.3	2.5%	48.9	8.2%	47.1	4.2%	45.3	0.3%
TC10	41.7	49.0	17.5%	46.5	11.6%	41.5	−0.5%	47.6	14.2%	45.8	9.8%	48.5	16.2%	45.8	9.9%	46.1	10.6%
TC12	46.6	51.4	10.3%	50.3	7.9%	46.1	−1.1%	49.5	6.3%	46.9	0.6%	50.8	9.0%	47.4	1.7%	45.7	−1.9%
TF1	32.7	33.1	1.3%	32.7	0.0%	32.7	0.0%	30.8	−5.9%	32.7	0.0%	32.7	0.1%	32.7	0.0%	32.7	0.0%
TF9	40.9	NA	0.0%	36.4	−11.0%	36.4	−11.0%	35.8	−12.4%	37.1	−9.4%	36.8	−10.1%	37.5	−8.4%	37.1	−9.4%
TF11	38.8	NA	0.0%	36.4	−6.2%	36.4	−6.2%	35.5	−8.6%	37.1	−4.5%	37.9	−2.5%	37.0	−4.7%	37.4	−3.7%
TF13	41.0	NA	0.0%	36.4	−11.2%	36.3	−11.4%	36.0	−12.1%	37.2	−9.1%	37.2	−9.3%	37.6	−8.3%	37.5	−8.5%
TF14	37.6	38.7	3.0%	37.7	0.3%	37.7	0.3%	34.3	−8.8%	37.6	0.0%	38.3	1.8%	37.8	0.7%	37.9	0.7%
		AVD	9.2%	AVD	8.4%	AVD	3.6%	AVD	9.2%	AVD	4.8%	AVD	8.8%	AVD	4.9%	AVD	5.2%

[a] The thermocouples error in the temperature measurement is less than 0.5 °C for temperatures lower than 50 °C and less than 0.8 0C for temperatures between 50 °C and 100 °C.

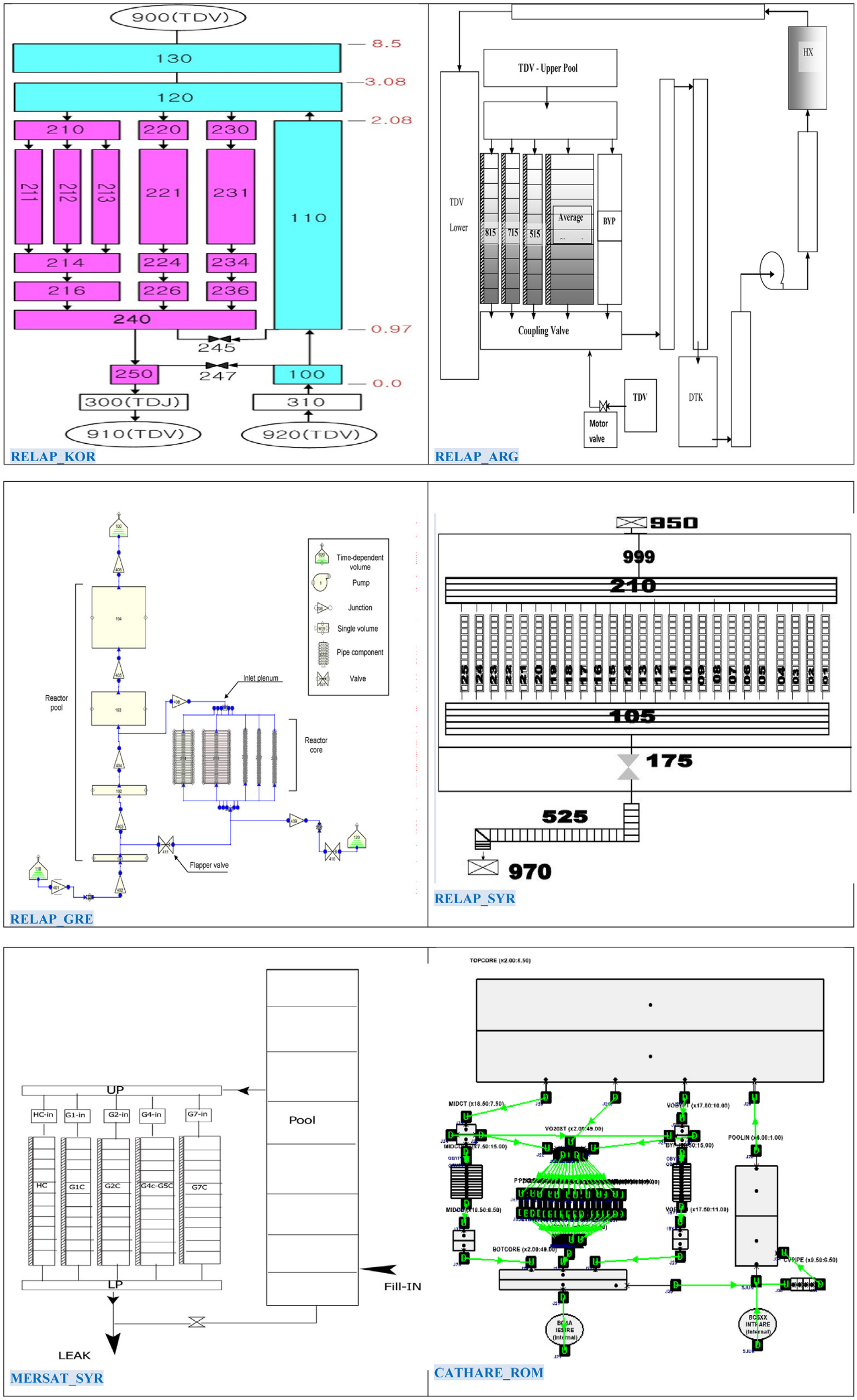

Fig. 6. Nodalization schemes of the TH codes applied for modelling IEA-R1 reactor.

where T_{exp} refers to the experimental temperature and T_{cal} is related to calculated values with each of the applied codes. n refers to the number of measurement points along the IFA which amounts to 14 temperature measurements of clad and coolant.

The resulting AVD shows best agreement for MTRCR-IEAR1(BRZ) with 3.3% followed by 4.8% for RELAP (KOR), 4.9% for MERSAT (SYR), 5.2% for RELAP (SYR), 8.4% for PARET (BRZ), 8.8% for CATHARE (ROM), 9.2% for RELAP (ARG) and RELAP (GRE)

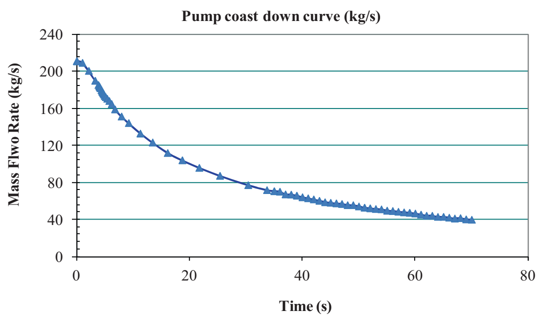

Fig. 7. Measured pump coast down curve during LOFA for IEA-R1

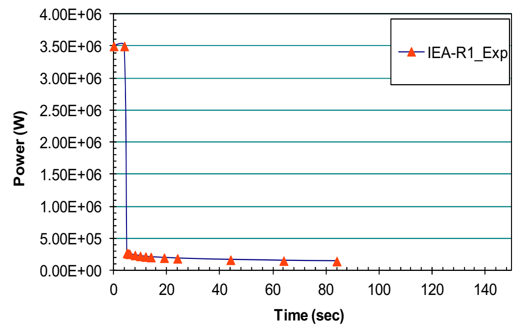

Fig. 8. Evolution of reactor power after reactor scram (decay heat curve).

In view of the fact that the expected thermal hydraulic phenomena under SS conditions that are dominated by single phase flow, are well modelled in all advanced computer codes, the observed discrepancy arises mainly from the experimental arrangement used to measure cladding temperatures in narrow channels. Most probably the weak contact of the thermocouple with the cladding can be the main source of uncertainty. Furthermore, the cladding temperature was measured with a disc inserted between adjacent fuel plates with the thermocouple welded at the disc centre (see Fig. 4). It is likely possible that this arrangement would cause contact resistance between the disc and fuel cladding resulting in measuring lower temperatures than exist in reality. In fact, the highest discrepancy is observed in case of central fuel plates. On the other hand, the measured coolant temperatures could be higher than the considered channel mean temperature as the location of thermocouple in the inserted disc in the narrow channel is measuring is nearby the wall where the coolant thermal layer has higher temperature than the assumed average value which is being calculated by the applied 1-D codes. This effect has been discussed with the experimental team that agreed with this interpretation. Finally, as no measurement for axial power density distribution of IFA is available, the IEA-R1 operator supplied calculated values based on the neutronic code CITATION (Umbehaun, 2012) (see also Fig. 5). This approach could add an additional source of uncertainty in view of the significant impact of this parameter on the axial temperature distribution.

4.2. LOFA benchmark results

The LOFA refers to the initiating event of loss of pump energy supply. The resulting decrease in core flow rate triggers the reactor scram once the flow rate reaches 93% of its nominal value (due to the protection criteria “Low Flow Rate”). Fig. 7 shows the experimental pump coast down curve where the flow rate decreases after the pump trip from its nominal value to about 20% in 70 s. After that time, the header (coupling valve) is decoupled and the reactor pool including the reactor core are no longer connected to the primary cooling loop.

By this experiment the LOFA has been started from an initial power level of 3.5 MW. The power distribution after reactor scram follows the time evolution of decay heat power that has been calculated by operator for the time up to 80 s after reactor scram (Fig. 8). For the remaining time (80–800 s) the employed codes use either built in heat decay tables or the international standard ANS94 (Torres et al., 2003).

The transient is initiated from the nominal steady state conditions of 3.5 MW rector power, 1.7 bar inlet pressure, 32.7 °C core inlet temperature and 211 kg/s total mass flow rate (corresponding to 6.27 kg/s for the IFA). The progression of the transient is summarized in the following event sequence:

- $t = 0$ s: pumps trip, and mass flow rate decreases according to Fig. 7,
- $t = 3$ s: reactor scram due to low flow (flow rate 93% of nominal),
- $t = 46$ s: opening of the coupling valve after decoupling the pump header (flow rate 27% of nominal),
- $t = \sim 100$ s onset of flow reversal (OFR).

To demonstrate the typical evolution of predicted normalized core mass flow rate during LOFA, the results of the codes MERSAT (SYR), RELAP (SYR) and RELAP (KOR) are presented in Fig. 9. Following the reactor operation at nominal condition the transient begins with the pump trip that occurs at $t = 0$ s. Once the flow rate reaches 93% of its nominal value (almost 3 s after the transient begins) the reactor scram is initiated. After reaching about 27% of nominal flow rate the pump header is decoupled and the coupling valve is opened (46 s after transient begin) so that the core outlet is directly linked to the reactor pool and the reactor core is no longer connected to the primary pump. In the following short time the forced downward flow through the core diminishes rapidly whereas at the same time the upward natural flow increases gradually and dominates finally inducing flow reversal from the downward forced circulation to the upward natural circulation (about 100 s after the transient begins). After a period of small oscillation the core mass flow of the prevailing natural circulation stabilizes at a certain small value. Up to the time point of opening the coupling valve the three codes predict the same behaviour. However, the flow reversal is initiated earlier by RELAP at almost 75 s from transient initiation compared to 100 s by MERSAT. In addition, after 250 s from transient initiation the natural circulation flow rate of MERSAT reaches about 2.7% of the nominal value (−5.5 kg/s) compared to 1.9% (−4 kg/s) for RELAP-SYR and 1.26% (−2.7 kg/s) for RELAP-KOR.

The predicted different flow rates of both RELAP models as well the predicted higher flow rate of MERSAT refers to the possible impact of the applied heat transfer correlation in the natural circulation regime which is being discussed later on.

The behaviour of flow reversal can be taken from Figs. 10 and 11 representing comparatively the predicted and measured time evolution of coolant inlet and outlet temperatures of IFA during the considered LOFA.

The outlet temperature evolution shows two peaks. The first small peak is observed shortly after the transient begins (pump trip) as a consequence of mass flow decrease whereas the reactor power remains at its initial value (during the first 3 s). Once the reactor scram is initiated the reactor power decreases faster than the mass flow and the coolant outlet temperature decreases abruptly from the first maximum to its minimum value. The measured outlet temperature reaches its first maximum of 37.8 °C at $t = 6$ s and decreases hereafter to a minimum of 33.3 °C at $t = 12$ s. After completing this phase and as a consequence of the continuing mass flow reduction (where at the same time the decay heat of medium and long lived fission products is decreasing slowly)

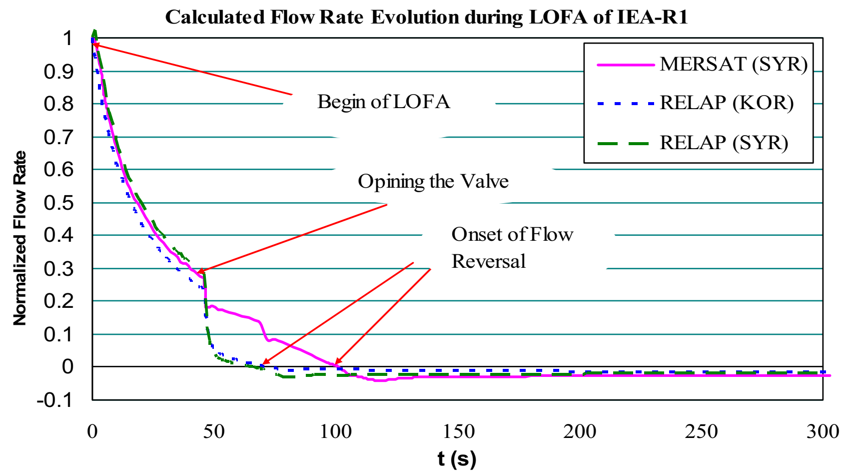

Fig. 9. Codes results for the evolution of relative mass flow of IEA-R1 core during LOFA.

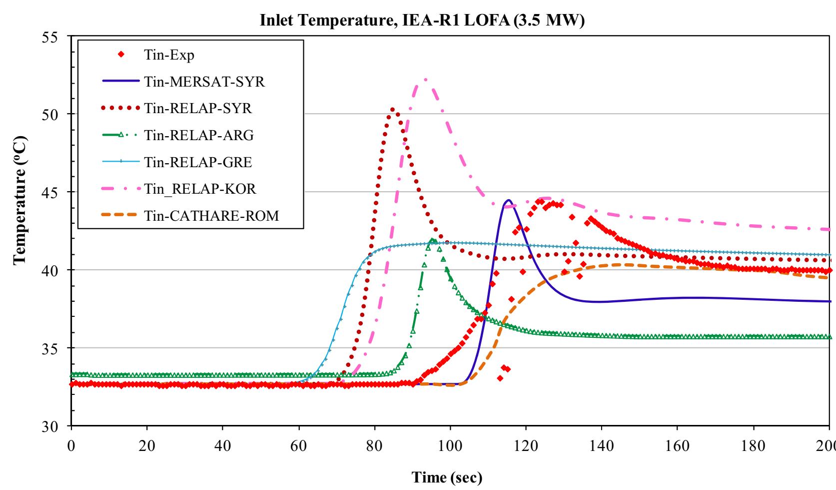

Fig. 10. Evolution of coolant inlet temperatures of IFA during LOFA (configuration 243).

the measured outlet temperature increases again and reaches its maximum of 38.65 °C (at 88 s). On the other hand and during the first 90 s of transient the inlet temperature remains constant at its initial value of 32.7 °C and prevails until the onset of flow reversal (OFR), where both temperatures interchange their positions. The outlet temperature (new inlet temperature) drops to the level of pool temperature (initial inlet temperature) whereas the inlet temperature (new outlet temperature) starts to increase and reaches a maximum of 44.4 °C after 123 s after transient initiation.

The observed spike of new outlet temperature is a direct consequence of flow stagnation at the outlet zone of fuel assembly immediately at the flow reversal. During this phase the transferred

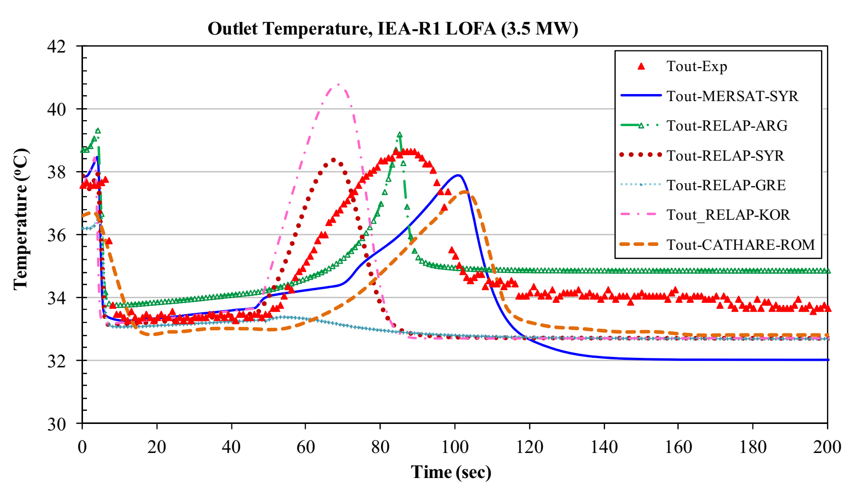

Fig. 11. Evolution of coolant outlet temperatures of IFA during LOFA (configuration 243).

Table 7
Comparison of measured and predicted coolant inlet and outlet temperature peaks and their time occurrences during LOFA of IEA-R1 (Configuration 243).

	T_{in}^{max} (°C)	$t_{in\text{-}max}$ (s)	Deviation		T_{Out}^{max} (°C)	t_{out}^{max} (s)	Deviation	
			T (%)	t (%)			T (%)	t (%)
Experiment	44.4	123	0.0	0.0	38.6	88	0.0	0.0
RELAP-ARG	42.0	95	−5.4	−22.8	39.1	85	1.3	−3.4
RELAP-GRE	41.8	102	−5.9	−17.1	33.4	54	−13.5	−38.6
RELAP-KOR	52.2	93	17.6	−24.4	40.8	68	5.6	−22.7
CATHARE-ROM	40.3	144	−9.2	17.1	37.3	104	−3.4	18.2
RELAP-SYR	50.3	85	13.3	−30.9	38.4	68	−0.6	−22.7
MERSAT-SYR	44.4	115.8	0.0	−5.9	37.9	101	−1.8	14.8

Deviation: relative difference to experiment for temperature (*T*) and related time (*t*).
The thermocouples error in the temperature measurement is less than 0.5 °C for temperatures lower than 50 °C and less than 0.8 °C for temperatures between 50 °C and 100 °C.

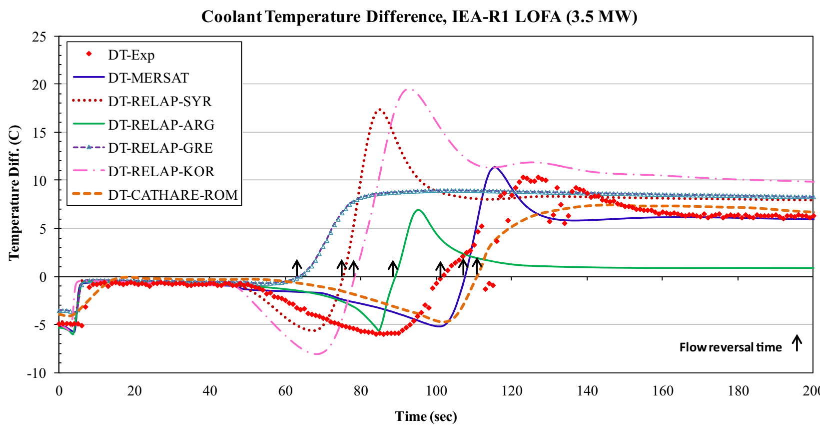

Fig. 12. Evolution of coolant temperature difference of IFA during LOFA (configuration 243).

decay power heats up the coolant along the fuel assemblies before establishing a fully developed natural circulation that assures the removal of remaining decay heat.

The qualitative comparison illustrates that all codes are able to simulate the trend of transient behaviour of coolant temperatures with different degrees of accuracy. The poorer agreement is observed for the cases of RELAP-GRE and CATHARE-ROM where the spikes of inlet and outlet temperatures are clearly underestimated. RELAP-KOR and RELAP-SYR show similar trend with conservative[1] estimation of inlet and outlet temperature spikes. RELAP-ARG predicts the spike of outlet temperature correctly whenever the time interval around the peak is very sharp. For the inlet temperature the spike is underestimated and its time occurrence is too early. MERSAT-SYR shows the best agreement for both temperatures spikes.

The quantitative comparison of measured and predicted inlet and outlet temperature peaks are presented in Table 7. The deviation of code predictions from experiment for both temperature peak values and their time occurrences are presented. The deviation varies between −5.4% and 17.6% for the inlet temperature peak and −31% and +17% for its onset time. For the outlet condition the deviation varies between −13.5% and +5.6% for outlet temperature peak and −38.6% and +18.2% for its onset time. The biggest discrepancy is observed for RELAP-GRE for both coolant inlet and outlet temperatures. For this case the expected peaks are less apparent. The best agreement is by MERSAT-SYR followed by RELAP-ARG.

Fig. 12 presents the resulting evolution of temperature difference between inlet and outlet. It depicts the flow reversal time – where the temperature difference vanishes – and gives indication about the prevailed natural circulation during the following time. One can see that after establishing the fully developed natural circulation, i.e. 150–200 s after transient initiation, both inlet and outlet temperatures decrease to a quasi constant level. The evolution trend of coolant temperature difference has direct impact on the clad temperature development demonstrated below. As presented in Table 8 the observed temperature differences between inlet and outlet temperature are 6.35 °C for experiment, 1 °C for RELAP-ARG, 8.3 °C for RELAP-GRE, 9.9 °C for RELAP-KOR, 9.3 for CATHARE-ROM, 6.65 °C for RELAP-SYR and 5.9 °C for MERSAT-SYR. MERSAT and CATHARE show the best agreement. RELAP predictions are relatively close to each other except in case of RELAP-ARG that shows remarkable low value of about 1 °C. This result indicates the important impact of user effect since RELAP results vary between the involved teams. The quantitative evaluation of these results is discussed in Section 4.3.

Figs. 13–15 present selected results of the benchmark calculation for the clad temperatures at 252.5 mm, 432.5 mm and 552.5 mm along the IFA for central and lateral fuel plates (compare with Fig. 2). The predicted codes results show quantitatively clear differences regarding second peak and its time occurrences. However, the qualitative trend of the time evolution is relatively similar characterized by first and second peaks followed by stabile final range. The most of predicted results of clad temperatures are conservative as the calculated peaks are higher than the experiment and their time occurrences are earlier. One exception is for MERSAT-SYR and CATHARE-ROM at 432.5 mm and at 552.5 mm where the time occurrences are delayed, besides for RELAP-ARG and CATHARE-ROM at 252.5 mm where the time occurrences are delayed and the temperature spikes are slightly underestimated. Remarkable is the time occurrence of clad temperature spike in

[1] Conservative means in this sense higher predicted temperatures and earlier time occurrences.

Table 8
Measured and predicted coolant temperature difference of IFA after establishing the fully developed natural circulation during LOFA.

	Experiment	RELAP-ARG	RELAP-GRE	RELAP-KOR	CATHARE-ROM	RELAP-SYR	MERSAT-SYR
$\Delta T_{coolant}$ (°C)	6.0	0.9	8.2	9.9	6.6	7.8	5.9
Deviation (%)	0	−85	37	65	10	30	−2

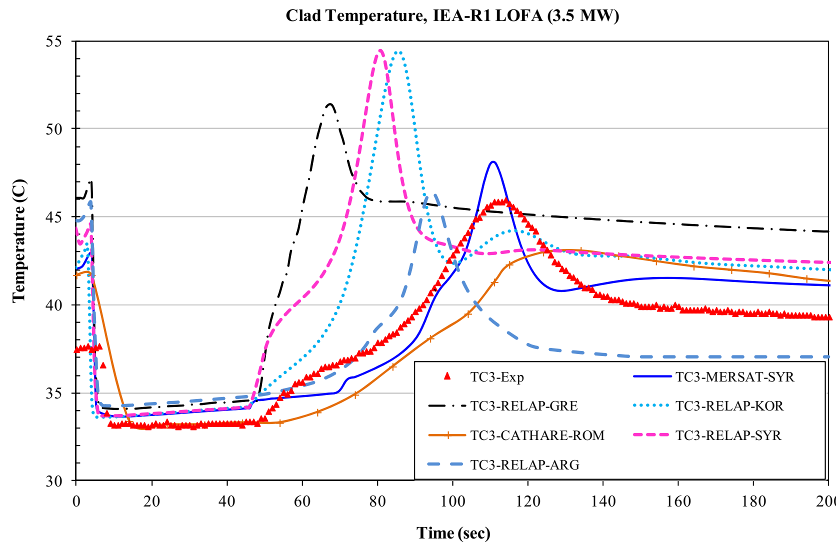

Fig. 13. Evolution of clad temperatures at 252.5 mm from the inlet of IFA (configuration 243).

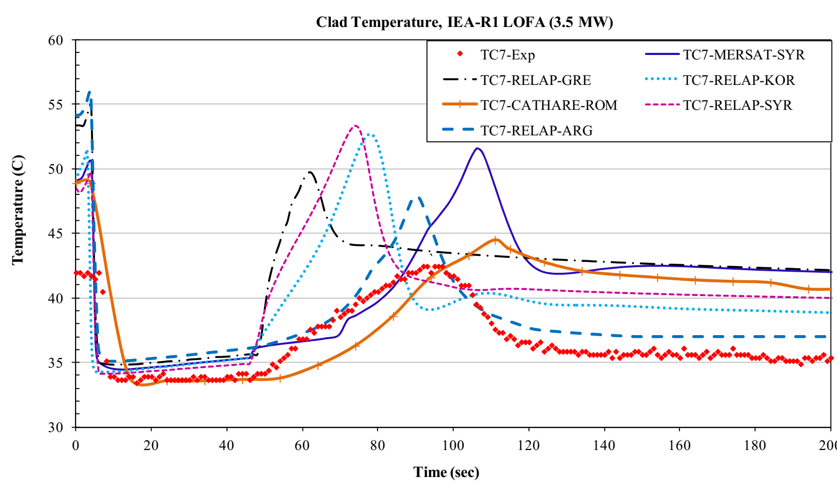

Fig. 14. Evolution of clad temperatures at 432.5 mm from the inlet of IFA (configuration 243).

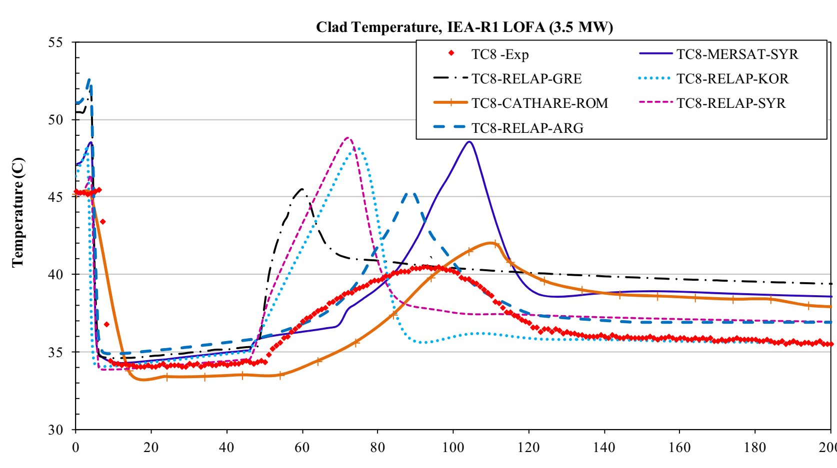

Fig. 15. Evolution of clad temperatures at 552.5 mm from the inlet of IFA (configuration 243).

Table 9
Deviation of calculated clad peak temperatures from the measurements during LOFA of IEA-R1 (configuration 243).

	TC2	TC3	TC4	TC5	TC6	TC7	TC8	TC10	TC12	*AVD*
Experiment	44.2	46.0	45.7	42.7	45.1	44.9	40.5	42.5	41.9	
RELAP-ARG	47.0	46.4	46.6	47.8	47.2	47.9	45.4	44.8	45.7	
Deviation (%)	6	1	2	12	5	7	12	6	9	*7*
RELAP-GRE	52.2	51.4	52.7	49.2	48.5	49.7	45.5	44.9	45.9	
Deviation (%)	18	12	15	15	7	11	12	6	9	*12*
RELAP-KOR	44.0	43.5	44.5	50.7	49.9	51.5	48.3	47.7	48.9	
Deviation (%)	0	−5	−3	19	11	15	19	12	17	*11*
CATHARE-ROM	42.4	43.1	42.8	43.4	44.1	44.5	42.0	42.5	42.9	
Deviation (%)	−4	−6	−6	2	−2	−1	4	0	2	*3*
RELAP-SYR	54.4	54.4	55.6	53.3	53.3	53.3	48.8	48.8	48.6	
Deviation (%)	23	18	22	25	18	19	20	15	16	*20*
MERSAT-SYR	49.0	48.1	49.2	51.3	50.6	51.5	48.5	48	48.7	
Deviation (%)	11	5	8	20	12	15	20	13	16	*13*

AVD: average relative deviation.

case of RELAP-GRE that appears about 50 s ahead of the experiment. The best qualitative agreement is observed by MERSAT-SYR followed by RELAP-ARG and CATHARE-ROM.

Table 9 summarizes the calculated peak clad temperatures in comparison with the experiment for all considered positions. The average relative deviation varies between +3% for CATHARE-ROM and +20% for RELAP-SYR. As depicted in Fig. 16 the majority of codes predictions are scattered above the full agreement line within a deviation of +20%. Thus, they overestimate the measurements and are therefore conservative from the view point of safety analysis. One exception is observed by CATHARE-ROM where the predicted peaks underestimate slightly the measurements.

4.3. *Relevant TH phenomena and impact of user effect*

As already mentioned, the considered LOFA analysis focuses on evaluating the TH phenomena taking place during the loss of downward forced coolant flow and the subsequent reversal to upward natural circulation with the provision of reactor shutdown without delay. The important TH parameters given by the evolution of coolant and clad temperatures and their peaks have been assessed and compared with available measurements of IFA. However, due to the important of LOFA for the safety analysis of research reactors, it is advisable to further discuss and compare further important TH parameters of the applied codes for which presently no measurement are available. This includes the time evolutions of flow rate, pressure drop across the core and HTC of IFA.

The evaluation of coolant flow rate and HTC help in explaining important TH phenomena related to flow reversal and natural circulation in the second phase of the transient. Discussing the simulation results of such parameters gives insight into the capability of the codes and enables performing of code-to-code validation in addition to addressing the aspect of user effect.

Fig. 17 presents the time evolution of flow rate through the IFA. The flow rate decrease during the first phase of downward forced convection shows good agreement among all codes. The OFR corresponds to zero flow rates showing the flow course change to upward direction. The predicted flow reversal times vary between 51.3 s for RELAP-GRE to 68 s for RELAP-SYR and RELAP-KOR and 84 s for RELAP-ARG. CATHARE-ROM and MERSAT-SYR show late onset time with about 90 s and 100 s respectively.

The flow reversal depends on the development of total pressure drop along the core (integral pressure drop). The total pressure drop consists of friction, form loss pressure drop (due to contraction and extraction losses at core inlet and outlet) and elevation term. Before analyzing the integral pressure drop it is helpful to assess the time evolution of local pressure along the IFA as depicted in Fig. 18 that shows exemplary the axial pressure distribution (given by CVs) at selected key time point for the case of MERSAT code. During the SS and right before starting the transient one can see that the prevailing downward flow leads to pressure decrease along the core (from core top to core bottom) as the negative friction and form loss pressure drop is higher than the positive elevation term. With progress of LOFA the coolant flow decreases gradually leading to declining the negative term of friction and form loss whereas the positive elevation term remain almost constant. Hence, the negative pressure gradient along the core lessens gradually and about 5 s after the start of transient the negative term of friction and form loss balances the elevation term and thus the pressure becomes nearly even (diminishing the pressure gradient) (Fig. 18). With the

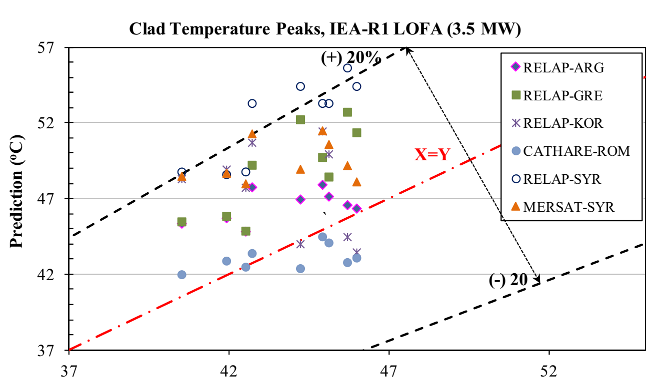

Fig. 16. Comparison of measured and predicted maximum clad temperatures during LOFA of IEA-R1 (configuration 243)

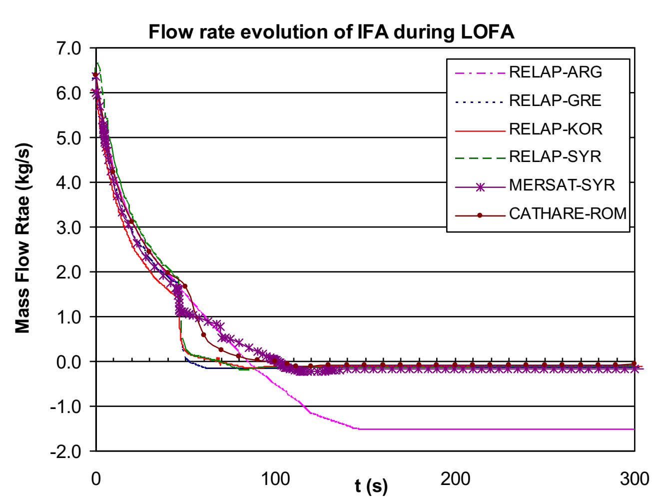

Fig. 17. Time evolution of mass flow rate of IFA during LOFA.

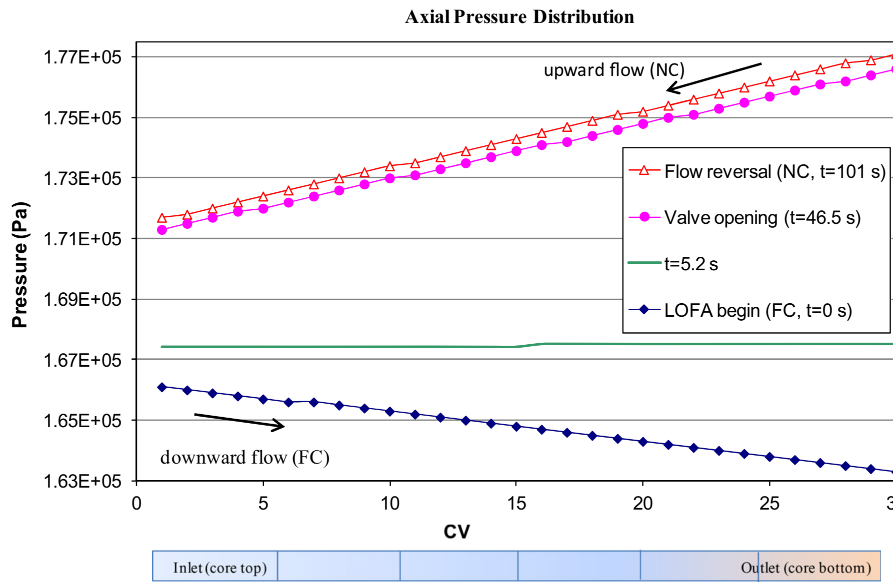

Fig. 18. Distribution of axial pressure drop during LOFA (MERSAT prediction).

successive declining of flow rate the pressure gradient becomes slightly positive (reverse pressure drop) and once the NC valve opens (at 46.5 s) the pressure gradient becomes clearly positive as the positive elevation term exceed by far the small negative friction term of diminishing flow rate which finally comes to stagnation. From this point on the flow reverses to upward direction forced by the onset of natural circulation being initiated by heating the coolant along the core. Finally, when the upward NC becomes fully developed the positive pressure gradient has constant slope and the coolant flows upward with almost constant low velocity dictated by the imposed post decay power of the fuel assemblies.

Making use of above elucidation the predicted evolutions of integral pressure drop of the applied codes are illustrated in Fig. 19. The pressure drop represents the pressure difference between core output and core inlet ($\Delta p = p_{out}^{corebot} - p_{inlet}^{corrtop}$). During the LOFA transient the integral pressure drop changes its sign from negative to positive (after about 5 s from transient begin, see Fig. 18). One can see the turn point at 46 s corresponding to NC valve opening time. In the following short time the forced downward flow through the core diminishes rapidly whereas at the same time the upward natural flow increases gradually inducing flow reversal from the downward forced circulation to upward natural circulation.

After the valve opening only small increase in the axial pressure is observed (Fig. 18) however no significant change is observed for the inversed integral pressure drop (Fig. 19). Besides, the pressure drop reaches its asymptotic constant level shortly after NC valve opening and the established reversed integral pressure drop corresponds mainly to the elevation term that dominates during the NC phase since friction and form loss terms are small due to the low NC velocity. Hence, the agreement between codes predictions during NC phase is good. On the other hand the observed discrepancy during the first FC phase corresponds to differences in calculating friction and form loss pressure drop. Further investigation of form loss coefficients (FLC) at inlet and outlet of IFA show their significant impact on the integral pressure drop during FC phase. Hence, FLC should be carefully estimated and validated by comparing the calculated integral pressured drop with real measurements for the nominal operation. This approach has been applied by all participating teams. Furthermore, the codes predictions show that the higher the inversed axial pressure gradient is the earlier is the flow reversal. This is the reason for the observed different flow reversal time.

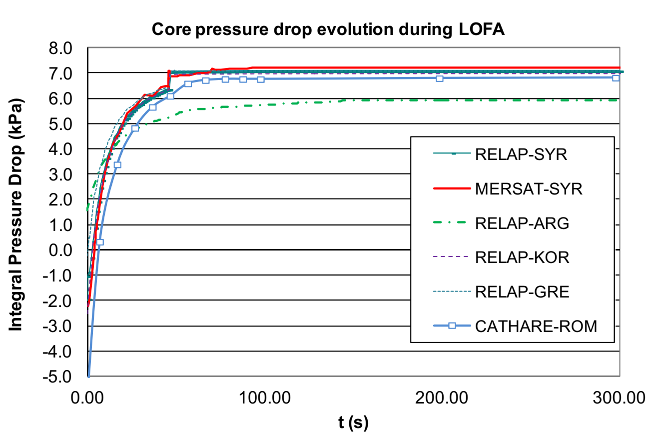

Fig. 19. Time evolution of integral core pressure drop during LOFA.

Fig. 17 shows that after a period of small oscillation the IFA mass flow of the prevailing natural circulation stabilizes at a certain small value. All codes predict the same general time evolution of mass flow and the final natural circulation flow rate is in the same range except for RELAP-ARG. The different trend of RELAP-ARG has been also observed for coolant temperature difference (see Figs 10–12). The predicted natural circulation flow rate depends on local HTC, post decay heat and the pressure drop components of friction and dimensionless form loss coefficient. To further analyze the results of natural circulation mass flow and its dependency on the prevailing TH conditions, the evolution of HTC is presented in Fig. 20. All codes follow the same trend during the forced convection phase except CATHARE that shows slightly higher HTC. However, during the NC phase RELAP-ARG and RELAP-KOR obviously predict very high HTC compared to other codes. The quantitative results of HTC for the fully developed NC are given in Table 10 that summarizes the main predicted TH parameters of the natural circulation established after flow reversal for all codes. HTC predicted by REALP-GRE and RELAP-SYR are in the same range and MESAT prediction is close to both. CATHARE predicts HTC value that is by 40% lower than by MERSAT. However, RELAP-ARG and RELAP-GRE show very high value of HTC that are respectively by factor 4 and 3 higher than by other RELAP predictions. Further evaluation and discussion with both teams indicate that in contrast to RELAP-SYR and RELAP-GRE

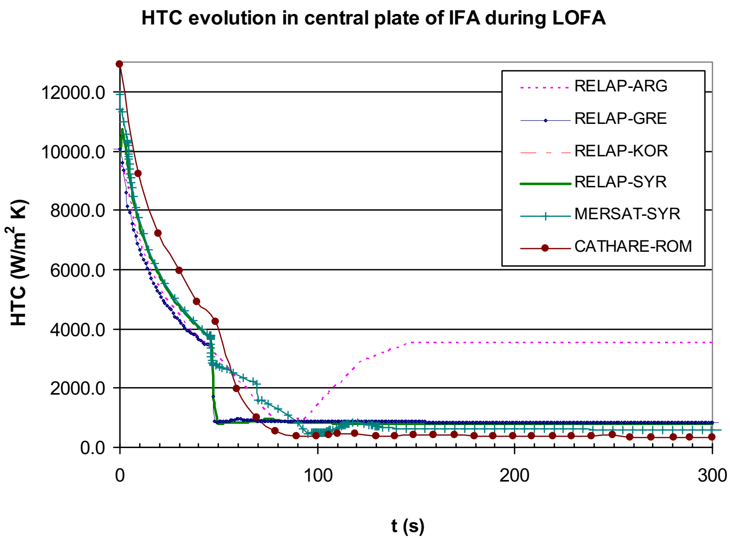

Fig. 20. Time evolution of HTC at position 552.5 mm of central plate of IFA.

Table 10
Predicted TH parameters of IFA after establishing the fully developed natural circulation during LOFA of IEA-R1.

	RELAP-ARG	RELAP-GRE	RELAP-KOR	RELAP-SYR	MERSAT-SYR	CATHARE-ROM
$\Delta T_{coolant}$ (°C)	0.9	8.2	9.9	6.6	5.9	7.8
G (kg/s)	1.524	0.137	0.108	0.124	0.166	0.073
$\dot{Q}_{coolant}$ (kW)	5.761	4.718	4.491	3.437	4.113	2.391
HTC (kW/m^2 K)	3.52	0.842	2.43	0.791	0.609	0.375
$T_{clad} - T_{col}$	0.8	4.6	1.37	3.4	5.3	3.47
$\dot{Q}_{HTC}$ (kW)	3.562	4.899	4.211	3.402	4.082	1.646
Flow reversal time (s)	84	51.3	68	68	100	90

where default RELAP option for calculating HTC in NC phase are used, both teams used the 102 set correlation in RELAP to calculate HTC which is devoted for narrow rectangular channels of Advanced Neutron Source Reactor Project in USA. Comparison test performed recently by project consolidator prove that option 102 deliver very high HTC compared to default RELAP option. Hence, 102 should be used only for TH conditions similar to those expected by ANS concept that is characterized by narrow channel and very high cooling velocity during the forced convection phase.

Plausibility check has been performed to verify the achieved predictions by comparing energy balance equation $\dot{Q}_{coolant}$ with the kinetic equation $\dot{Q}_{HTC}$ (integral heat transfer equation) along the IFA:

$$\dot{Q}_{coolant} = G \cdot c_p \cdot \Delta T_{coolant}$$

$$\dot{Q}_{HTC} = A \cdot HTC \cdot (T_{clad} - T_{col})$$

where G is mass flow rate, A is total heat transfer area of IFA, c_p is coolant heat capacity, $\Delta T_{coolant}$ coolant temperature difference between outlet and inlet of IFA. T_{cld} and T_f refer to the average clad and coolant temperatures for the three sub-channels and along the IFA. Table 10 presents selected TH parameters together with the verification of both energy equations. It can be seen that both are close to each others whereas $\dot{Q}_{HTC}$ is slightly lower than the exact integral value of heat balance ($\dot{Q}_{coolant}$) due to the fact that its calculation based on average values for HTC, clad and coolant temperatures. Due to overestimated flow rate for RELAP-ARG the heat balance is by 40% higher than $\dot{Q}_{HTC}$ and the coolant heat rate of 0.9 °C is significantly lower than the measurement of 6 °C (see Table 8). For CATHARE-ROM the underestimated HTC led to underestimating $\dot{Q}_{HTC}$ by 30% compared to $\dot{Q}_{coolant}$.

It is obvious from Table 10 that due to the overestimated HTC in case of RELAP-KOR and RELAP-ARG the predicted $T_{clad} - T_{col}$ is low compared to others and consequently the calculated clad temperature is underestimated (see Fig. 13).

Fig. 17 presents the time evolution of flow rate through the IFA. The flow rate decrease during the first phase of downward forced convection shows good agreement among all codes. The OFR corresponds to zero flow rates showing the flow course change to upward direction. The predicted flow reversal times vary between 51.3 s for RELAP-GRE to 68 s for RELAP-SYR and RELAP-KOR and 84 s for RELAP-ARG. CATHARE-ROM and MERSAT-SYR show late onset time with about 90 s and 100 s respectively.

5. Conclusions and recommendations

Special thermal hydraulic measurements have been performed in the Brazilian RR IEA-R1 using an instrumented fuel element assembly (IFA) that was placed in two different core positions. The acquired measurements cover coolant and cladding temperatures as well flow rate during loss of flow transient (LOFT). The measurements have been used by five independent teams to benchmark the TH codes RELAP5, MERSAT, CATHARE and PARET. The benchmark results indicate that the predicted evolution of coolant and cladding temperatures follow in general the overall trend of the measurements. However, the predicted clad temperature peaks overestimate the measurements by a maximum of about 20%. Furthermore, the time occurrences of the peak temperatures are generally earlier than the experimental results. In view of the importance of clad peak temperature for the safety analysis, the overestimated predictions support the tendency towards conservative results. Temperature predictions (coolant and cladding) have much faster gradients than the measurement.

The additional code-to-code comparison regarding integral pressure drop during LOFA show good agreement among the codes despite the differences in the applied modelling approaches. However, discrepancies are observed regarding onset of flow reversal time as well mass flow rate and HTC during natural circulation phase. The selection of option 102 for HTC in RELAP by two teams lead to overestimation of natural convection HTC compared to the default option 101 that show good agreement among three RELAP users besides its good agreement with MERSAT result. CATHARE result for both HTC and flow rate during NC are underestimated compared to RELAP (with default HTC option) and MERSAT.

Since the developed CATHARE model of IEA-R1 is comprehensive its predicted low HTC during NC leads to the recommendation to compare the implemented HTC correlation that of RELAP and MERSAT for possible verification and improvement.

The impact of user effect on the benchmark results has been assessed for RELAP code by comparing the efforts of 4 teams. The comparison of the input files show similarity in the main input parameters related to IFA although various simplification approaches are adopted for the remaining fuel elements and primary loop components. The results prove not to be sensitive to different axial nodalization of IFA for the range of 15–30 CV. SS results seem to be very close despite small differences attributed to differences in defining axial power distribution and radial power factor and flow distribution of internal channels of IFA. However, discrepancies are observed during natural circulation phase of LOFA mainly caused by modelling of pump coast down curve, the applied post decay heat tables and even the employed details in modelling the primary loop including reactor pool.

RELAP code has been used by 4 teams. Hence, to account for detailed user effect impact on the benchmark results RELAP input files of the various users should be exchanged and compared. This may assist to eliminate input errors, improve modelling approach and understand the origin of some of the observed differences by performing sensitivity analyses.

It is worthy to mention that the quality of the employed experimental data is not fully satisfactory due to the measurement limitation to clad and cooling temperatures and the discussed deficit in the procedure of temperature measurement. Hence, the final decision to rely upon such measurements to validate the employed codes regarding the addressed TH phenomena requires considering following recommendations:

- Special attention should be given when measuring coolant and clad temperatures. Specifically, this should include a validation that the thermocouples are indeed measuring the required quantity i.e. clad temperature or coolant temperature at a well specified location. In the case of the coolant temperature there is a temperature gradient near the surface of the fuel plate and this must be considered when locating the thermocouple such narrow channels.
- The time response of the thermocouples should be verified and stated in the benchmark.
- The impact of the instrumentation of IFA on the thermal hydraulic conditions and hence the parameters being measured should also be carefully considered and quantified if possible. Hence, uncertainties analysis of experimental data could improve the data quality and allow sensitivity analyses to be performed.
- Verification of the flow rate distribution between the IFA channels is important and should be performed for the particular experiment or shown to be independent of core position.
- Additional measurements should be considered in future activities to include mass flow rate and pressure drop evolution over the time of the considered transient.

Acknowledgments

This work was performed as part of IAEA's Coordinated Research Project (CRP) on innovative methods in research reactor analysis: Benchmark against experimental data on neutronics and thermal hydraulic computational methods and tools for operation and safety analysis of research reactors. The authors would like to express their appreciation to the International Atomic Energy Agency (IAEA) for the technical and financial support. They also thank Dr. C.M. Allison (Innovative Systems Software LLC, USA) who enabled the participating teams the cost free application of RELAP code for the exclusive application during the CRP.

References

Benchmark analysis for RR. 2014. IAEA TC-Doc (under publication).
Bestion, D., 2008. System Code Models and Capabilities. THICKET, Session III, Paper 06.
D'Auria, F., Bousbia-Salah, A., Galassi, G.M., Vedovi, J., Reventós, F., Cuadra, A., Gago, J.L., Sjöberg, A., Yitbarek, M., Sandervag, O., Garis, N., Anhert, C., Aragonés, J.M., Verdù, G., Mirò, R., Ginestar, D., Sánchez, A.M., Maggini, F., Hadek, J., Macek, J., Ivanov, K., Uddin, R., Sartori, E., Rindelhardt, U., Rohde, U., Frid, W., Panayotov, D., 2004. Neutronics/Thermal Hydraulics Coupling in LWR Technology, Vol. 2 – State-of-the-Art Report. OECD (NEA No. 5436).
D'Auria, F., Mazzantini, O., 2010. The best-estimate plus uncertainty (BEPU) challenge in the licensing of current generation of reactors, IAEA-CN-164-4S08.
Database of Research Reactor Benchmarks, 2014. Description of facilities, associated experiments and data. IAEA TC-Doc. (under publication).
Day, S.E., Chatzidakis, S., 2012. SPERT-IV consolidation status, 4th RCM Meeting , IAEA, Vienna, Austria, 17–21 December.
Hainoun, A., Alissa, S., 2005. Full-scale modeling of the MNSR reactor to simulate normal operation, transients and reactivity insertion accidents under natural circulation conditions using the thermal hydraulic code ATHLET. Nucl. Eng. Des. 235 (1), 33–52.
Hainoun, A., Schaffrath, A., 2001. Simulation of subcooled flow instability for high flux research reactors using the extended code ATHLET. Nucl. Eng. Des. 207 (2), 163–180.
Hainoun, A., Hicken, E., Wolters, J., 1993. ATHLET-extension for application research reactors. In: Proceedings of Annual Meeting of Nuclear Technology 1993, Koeln, Germany.
Hainoun, A., Hicken, E., Wolters, J., 1996. Modelling of void formation in the subcooled boiling regime in the ATHLET code to simulate flow instability for research reactors. Nucl. Eng. Des. 167 (2), 175–191.
Hainoun, A., Ghazi, N., Alhabit, F., 2008a. Simulation of LOFA and RIA for the IEA-R1 research reactor using the code MERSAT. Ann. Nucl. Energy 35 (11.), 2093–2104.
Hainoun, A., Alhabit, F., Ghazi, N., 2008b. Modification and validation of the natural heat convection and subcooled void formation models in the code PARET. Ann. Nucl. Energy 35 (3), 395–403.
Hamidouche, T., Bousbia-Salah, A., 2006. RELAP5/3.2 assessment against low pressure onset of flow instability in parallel heated channels. Ann. Nucl. Energy 33, 510–520.
Hamidouche, T., Bousbia-Salah, Al Khider, S., D'Auria, F., 2008. Overview of accident analysis in nuclear research reactors. Progr. Nucl. Energy 50, 7–14.
Hamidouche, T., Bousbia-Salah, Al Khider, S., Yazid Mokeddem, M., D'Auria, F., 2009. Application of coupled code technique to a safety analysis of a standard MTR research reactor. Nucl. Eng. Des. 239 (10), 2104–2118.
G. Lavialle – CATHARE V25_1 Users Manual, SSTH/LDAS/EM/2005-035.
Noel, B., 2011. DEN platform for thermal hydraulic simulation of reactors with focus on system CATHARE code. In: 3rd RCM of IAEA CRP1496, 5–9 December, Aix-en-Provence, France.
December 2001. RELAP5/MOD3.3 Code manual volume I: Code structure, system models, and solution methods. Nuclear Safety Analysis Division, Office of Nuclear Regulatory Research U.S. Nuclear Regulatory Commission, Information Systems Laboratories, Inc., Rockville, Maryland Idaho Falls, Idaho.
December 2001. RELAP5/MOD3.3 Code manual volume IV: Models and correlations. Nuclear Safety Analysis Division, Office of Nuclear Regulatory Research U.S. Nuclear Regulatory Commission, Information Systems Laboratories, Inc., Rockville, Maryland Idaho Falls, Idaho.
Obenchain, C.F., 1969. PARET-A program for the analysis of reactor transients. Idaho National Engineering Laboratory (Report IDO-17282).
Omar, H., Ghazi, N., Alhabit, F., Hainoun, A., 2010. Thermo-hydraulic analysis of Syrian MNSR research reactor using RELAP5/Mod3.2 code. Ann. Nucl. Energy 240 (5), 1132–1138.
2008. Safety Reports Series No. 55: Safety Analysis of Research Reactors. IAEA's, Vienna.
Torres, W.M., Umbehaun, P.E., Andrade, D.A., Souza, J.A.B., 2003. A MTR fuel element flow distribution measurement, preliminary results. In: International Meeting on Reduced Enrichment for Research and Test Reactors, Chicago, Illinois, October 5–10.
Umbehaun, P.E., 2012. Description of IEA-R1 reactor.
Umbehaun, P.E., Delvonei, D., Torres, W., Filho, W., 2012. Final Report for the Coordinated Research Project 1496. IPEN-CNEN, Brazil.

Glossary

AECS: Atomic Energy Commission of Syria
ANL: Argonne National Laboratory
ANS: American Nuclear Society
ARG: Argentina
AVD: average relative deviation
CRP: coordinated research project
CV: control volume
FC: forced convection
FLC: form loss coefficient
GRE: Greece
HTC: heat transfer coefficient
IFA: instrumented fuel assembly
IFE: instrumented fuel element
KOR: Korea (Republic of)
LOCA: loss of coolant accident
LOFA: loss of flow accident
MTR: material testing reactor
NC: natural circulation/convection
OFR: onset of flow reversal
RIA: reactivity insertion accident
ROM: Romania
RR: research reactor
SS: steady state
SYR: Syria
SYS-TH: system thermal hydraulic
TH: thermal hydraulic